

Design of a Two-Stage PPT for Cubesat Application

IEPC-2009- 244

*Presented at the 31st International Electric Propulsion Conference,
University of Michigan • Ann Arbor, Michigan • USA
September 20 – 24, 2009*

M. Coletti¹
Mars Space Ltd., Southampton, SO16 3QD, United Kingdom

R. Intini Marques² and S. B. Gabriel³
University of Southampton, Southampton, SO17 1BJ, United Kingdom

Cubesats are one of the fastest growing sectors in the space industry, allowing for cheap access to space. ESA has funded a project involving Clyde Space Ltd, Mars Space Ltd and the University of Southampton to develop an adaptation of a Two-Stage PPT to perform drag compensation for a Cubesat platform, with the aim of doubling the time needed for the Cubesat to naturally de-orbit (hence doubling its lifetime). In this paper the mission requirements and the design process of this Two-Stage PPT will be presented.

Nomenclature

| | | |
|------------|---|---------------------------------------------|
| A | = | area of propellant exposed to the discharge |
| C | = | capacitance |
| d_{el} | = | electrode length |
| d_{prop} | = | propellant bar width |
| E | = | energy |
| h | = | electrode spacing |
| I_{bit} | = | impulse bit |
| I_{sp} | = | specific impulse |
| I_{tot} | = | total impulse |
| L_{prop} | = | propellant bar length |
| L_0 | = | initial inductance |
| L' | = | inductance change per unit length |
| m' | = | linear of gaseous density |
| P | = | power |
| R | = | resistance |
| t | = | electrode thickness |
| w | = | electrode width |
| α | = | dynamic impedance parameter |
| Δm | = | ablated mass |
| ψ | = | critical resistance ratio |

Subscripts

| | | |
|---|---|------------------------------------------|
| 1 | = | relative to the first set of electrodes |
| 2 | = | relative to the second set of electrodes |

¹ Researcher, Mars Space Limited, michele.coletti@mars-space.co.uk

² Research Fellow, Astronautics Research Group, intini@soton.ac.uk

³ Professor of Aeronautics and Astronautics and Head of the Astronautics Research Group, sbg2@soton.ac.uk.

Copyright © 2009 by Michele Coletti. Published by the Electric Rocket Propulsion Society with permission.

I. Introduction

CUBESATS are normally launched into sun-synchronous or LEO orbits with an altitude of about 600-650 km. They are currently limited by their lack of orbit control and their lifetime is therefore determined by the natural, drag-induced, de-orbiting.

Clyde Space Ltd, Mars Space Ltd and the University of Southampton have started a study funded by the ESA ITI program to adapt a Teflon-fed High Frequency Burst PPT to a 3U Cubesat with the aim of doubling its lifetime.

Ablative Pulsed Plasma Thrusters (PPTs) have been chosen as propulsion subsystem thanks to their high scalability in terms of geometry, power input and performance and also to their high reliability and easiness of control. Despite their simplicity and reliability PPTs are affected by a very low efficiency, of the order of 10% [1]. This low efficiency is partially due to the very poor propellant utilization inside this thruster; typically only 40-60% of the propellant contributes to produce significant impulse [1-3].

The cause of the PPT poor propellant utilization has been identified as Late-Time Ablation (LTA) [2, 3]. LTA is the sublimation of propellant that takes place after the main discharge, due to the propellant (usually Teflon) temperature being above its sublimation point. The LTA produces a low speed gas and macro particles that do not contribute significantly to the thrust [1].

A possible improvement on current PPT design, aimed at solving this problem, has been proposed with the concept of the Two-Stage Pulsed Plasma Thruster (TS-PPT), including the High Frequency Burst Pulsed Plasma Thruster (HFB-PPT) [4-6].

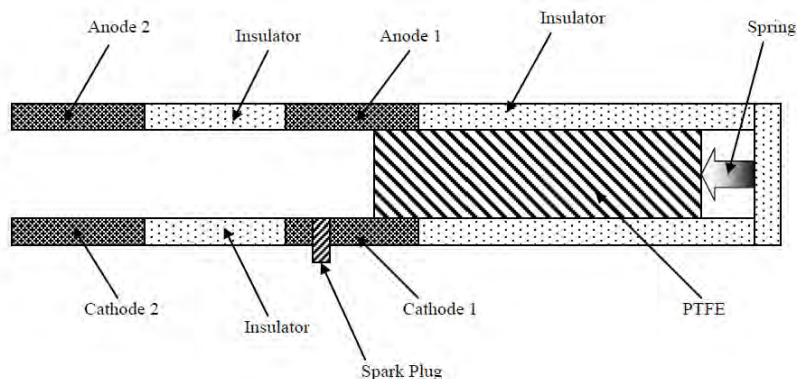


Figure 1: Diagram of a HFB-PPT [4].

In a HFB-PPT the LTA is accelerated, hence improving the propellant utilization efficiency[5, 6]. This is accomplished by employing a mechanism that involves firing secondary discharges from a secondary set of electrodes further along the discharge chamber, synchronised to coincide with the arrival of ablated fuel.

The goal of this study is therefore to develop a HFB-PPT able to double the lifetime of a Cubesat and, at the same time, to collect data that will help to better understand the functioning of a HFB-PPT, allowing for its future optimization. Considering the tight mass budget expected for a Cubesat application the output of the project will gain even more importance in the future development of HFB-PPTs. In fact, if the experimental investigation will show encouraging performances of this kind of thruster even when constrained by a limited mass and volume budget, it is arguable that with less stringent constraints the performance level could be further improved.

In this paper the design process of the HFB-PPT discharge chamber will be extensively presented.

II. Requirements

In this section the requirements that must be met by the HFB-PPT in terms of mass, dimensions, power and performance will be presented.

The thruster and its electronics will be mounted on a PC104 standard PCB card that is normally adopted by the Cubesat Kit bus with a maximum volume of 90×90×27 mm. Since the PCB cards are normally mounted horizontally the thrust direction will be along the 27mm direction. Considering that a PC104 card has dimensions of 90.17×95.89×1.6 mm the maximum allowable length of the discharge chamber of the HFB-PPT will be 25mm.

Given the Cubesat tight mass budget, the mass of the whole thruster assembly including electronics, capacitors and propellant will be limited to 120g (without margins); this translates into a total maximum mass of 150g including a 25% mass margin. Due to the limited mass available, the propellant (Teflon[®]) mass will be limited to 5g.

The power available is limited due to the limited solar panel extension on board a Cubesat: a maximum limit has been fixed at 0.3 W of average power consumption.

The thruster will be required to compensate the drag induced de-orbiting for a period of at least 3 years at a nominal altitude of 600 km. Considering that at this altitude a Cubesat lifetime is about 3 years, if the thruster will meet the performance requirement, the Cubesat lifetime will be extended to 6 years. Assuming a drag coefficient of 2.2 on a 3U cubesat the total impulse needed to fully compensate three years of drag will be 28.4Ns that, considering a propellant mass of 5g, translates into an average specific impulse of 570 s.

A table summarizing the thruster requirements is reported below.

| | | | |
|----------------------------------------|------------|-------------------------------------|--------|
| Maximum volume | 90×90×25mm | Total impulse | 28.4Ns |
| Maximum mass (including 25% margin) | 150g | Average power | 0.3W |
| Maximum thruster length | 25mm | Minimum average Specific Impulse | 570s |

III. Thruster design

In this section the thruster design will be presented. Firstly the design of the first stage will be presented (A), then the expected first stage performance will be analyzed and the performance required from the second stage derived (B). After this, the design of the second stage will be presented (C) and finally the spark plug design will be reported (D).

A. First Stage Design

The design of the first stage of the HFB-PPT will be now presented. The focus will be on maximizing its performance to ideally be able to meet the requirements only with the first stage. Hence, since the propellant mass is fixed (5g), we will try to maximize the specific impulse. This choice was made as a safety measure, due to the fact that up to now no direct measurements have been made relatively to the increase in thrust/specific impulse of an HFB-PPT. Nevertheless, calculations based on experimental current measurements indicate that significant improvements in specific impulse are possible [6].

1. Breech fed versus side fed

The first design choice to be made is between a breech-fed and a side-fed configuration. According to the Requirements section the thruster discharge chamber maximum length is 25 mm. Since the total available length is already small, and considering that the choice of a breech-fed configuration would further reduce the available length to allow for propellant storage, our baseline design will be based on a side-fed configuration.

We can now choose between two different propellant bar geometry: straight bars or curved bars. Straight bars are easier to manufacture and easier to feed into the thruster discharge chamber, allowing in our case a maximum propellant bar length of 90mm minus the discharge chamber width; curved bars, instead, are more complicated to manufacture, they require a circular spring to be fed to the thruster but, assuming to have enough volume available, allow a much bigger maximum propellant length.

Considering that we want to keep the design as simple as possible and that curved propellant bars would create additional difficulties in the positioning of the electronics around the discharge chamber our baseline choice will be to use straight propellant bars.

2. Electrode dimensions

The design will now move forward to the definition of the propellant bar, electrode dimensions and discharge energy. In many of the past works involving both side-fed and breech-fed PPTs [1, 7-10] one of the main parameters found to affect the thruster performances in terms of propellant consumption and specific impulse is the ratio of the discharge energy to the propellant area exposed to the discharge. In particular it has been found that higher energy per area ratio tends to deliver higher values of Isp.

Table 2. Performance of various PPTs [1]

| | Energy [J] | Isp [s] | Ibit [$\mu\text{N/s}$] | Ibit/E [$\mu\text{Ns/J}$] | $\Delta m/E$ [$\mu\text{g/J}$] | Δm [μg] | A [cm^2] | E/A [J/cm^2] | η [%] |
|---------------------------|---------------|------------|-----------------------------|--------------------------------|-------------------------------------|---------------------------------|------------------------|----------------------------|---------------|
| LES-6 (breech-fed) | 1.85 | 300 | 26 | 14 | 4.8 | 8.9 | 2.69 | 0.69 | 2 |
| SMS (breech-fed) | 8.40 | 450 | 133 | 15 | 3.4 | 28.5 | 7.32 | 1.15 | 3.7 |
| TIP-II (breech-fed) | 20 | 850 | 375 | 19 | 2.3 | 46 | 8.07 | 2.48 | 7.6 |
| China Lab (breech-fed) | 23.9 | 990 | 448 | 19 | 1.9 | 45.4 | 8.57 | 2.79 | 9.2 |
| LES-8/9 (breech-fed) | 20 | 1000 | 297 | 15 | 1.5 | 30 | 6.25 | 3.20 | 7.3 |
| Mitlab (side-fed) | 20 | 600 | 454 | 23 | 2.8 | 56 | 13.02 | 1.54 | 9.2 |
| Mipd3 (side-fed) | 100 | 1130 | 2250 | 23 | 2 | 200 | 46.51 | 2.15 | 12.6 |
| Millipound (side-fed) | 750 | 1210 | 22300 | 30 | 2.5 | 1875 | 67.69 | 11.08 | 17.7 |

In our design the minimum propellant surface area is limited by the maximum length of the propellant bars (since the propellant mass is fixed to 5 g) whereas the maximum energy is limited by the capacitor weight and by the minimum allowable shot frequency.

Considering the data reported in Table 2 and the limited power availability our baseline choice will be to use $E/A=2 \text{ J/cm}^2$. This choice will be further justified later on.

The electrode dimensions and material will be chosen to minimize mass and electrical resistance and to maximize the inductance variation per unit length. We have chosen to use a copper-tungsten (70% W – 30% Cu) alloy to build the electrodes. This material has been chosen for its low electrical resistivity (37 n Ωm) and for its good mechanical and thermal properties and reduced erosion rates [11, 12].

As reported in many studies regarding the PPT functioning [4, 9] the electromagnetic acceleration component and efficiency are found to be respectively proportional to the inductance variation per unit length L' and to the ratio between the inductance variation during the discharge and the initial discharge circuit inductance $\Delta L/L_0$. To maximize the first stage performance we will then try to minimize L_0 and maximize L' .

To minimize the initial inductance we will design the thruster to allow the capacitors to be mounted as close as possible to the discharge chamber whereas to maximize the value of L' we will act on the electrodes dimensions.

The inductance variation per unit length can be calculated as [13]

$$L' = 0.6 + 0.4 \ln \frac{h}{w+t} \quad [\mu\text{H}/\text{m}] \quad (1)$$

or according to another approach using a conformal mapping technique [14] the value of L' can be plotted for various h/w ratios.

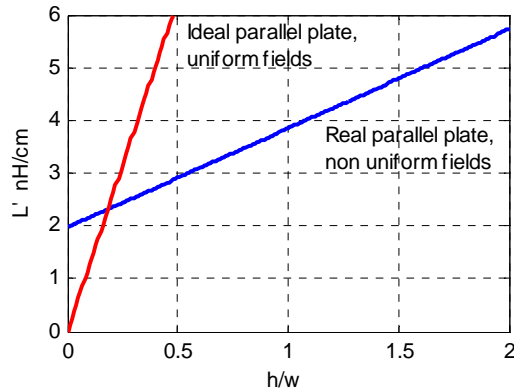


Figure 2: Inductance per unit length trend with h/w ratio [12].

According to both approaches to maximize L' the electrode spacing must be increased and the electrode width and thickness decreased. However if the value of h/w is too high important non uniformities may arise in the electromagnetic field, thus reducing the acceleration process efficiency [15]; moreover an increase of h will also increase the resistance of the plasma, hence reducing the current and consequently reducing the electromagnetic impulse bit. Considering what has been said above an h/w ratio equal to 2 will be chosen for the design of the HFB-PPT first stage.

Considering that the values of h in PPTs with shot energy in the joule level are normally of the order of one to some centimeters we will chose an electrode spacing h of 1cm and consequently an electrode width of 5 mm. The electrode thickness will be fixed to a value of 2 mm to assure mechanical resistance, low electrical resistance and limited mass.

3. Propellant bar dimensions and shot energy

The height of the propellant bars will be slightly more than the electrode spacing, to allow the blocking of the propellant on the electrode shoulder: the propellant bar height will be then 12 mm. It is left to determine the propellant bar length (L_{prop}) and width (d_{prop}). These two values cannot be chosen arbitrarily since the propellant mass should be equal to 5g and since the value of d_{prop} will influence the area of the propellant face exposed to the discharge, hence influencing the value of the E/A ratio. In the next figure the values of L_{prop} and d_{prop} for different values of E/A and discharge energy are reported.

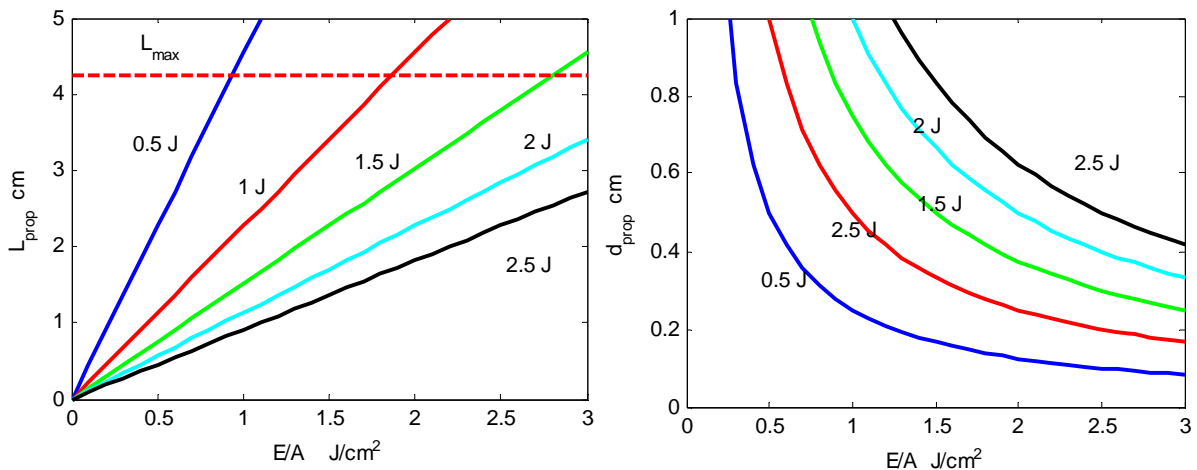


Figure 3: L_{prop} and d_{prop} trend with E/A for different values of the shot energy E_s .

As can be seen from Figure 3 the trends of L_{prop} and d_{prop} with shot energy and E/A are of opposite nature. An increase in E/A causes an increase in L_{prop} and a decrease in d_{prop} whereas an increase in the shot energy has the opposite effect.

Considering that the maximum length in Figure 3 does not take into account the space taken by the feeding springs and by any structural support that the propellant needs, that the average power available is 0.3W and that the total thruster length should be less than 25 mm, we have decided to minimize the value of d_{prop} while maintaining a reasonable value of both E and E/A .

Our baseline choice will be then to use 1.5 J of energy per shot in the first stage with an energy over area ratio of 2 J/cm^2 . This will give us a length of the propellant bars of 3.1 cm on each side of the thruster and a d_{prop} of 3.5 mm.

The last parameter to be determined to complete the design of the first stage is the length of the electrode d_{el} ; considering that, as for d_{prop} , this value is limited by the total length available for the thruster, we will fix this to 0.5 cm. To reduce carbon deposition on the thruster walls [6], that might lead to electrode short-circuiting, we will also introduce a divergence in the thruster side wall of 10° with respect to the thruster axis.

In conclusion the design of the first stage can be summarized as follows

| | | | |
|-----------------------------------|--------|----------------------------|--------------|
| Teflon [®] bar geometry | Linear | Electrode length, d_{el} | 0.5cm |
| Teflon [®] mass | 5g | Electrode spacing, h | 1cm |
| Propellant bar length, L_{prop} | 3.1cm | Electrode width, w | 0.5cm |
| Propellant bar height, h | 1.2cm | Electrode thickness, t | 3mm |
| Propellant bar width, d_{prop} | 0.35cm | Electrode material | 30% Cu 70% W |
| Shot energy, E | 1.5J | Sidewall divergence | 10° |

B. Performance Analysis

We will now analyze the performance that may be expected from the thruster and we will compare it with the mission requirements. We will start by analyzing the first stage and then we will move on to the derivation of the performance required from the second stage.

The first stage performance will be analyzed assuming two different values of the I_{bit_1}/E_1 ratio, $23 \mu\text{Ns/J}$ (typical value for a side fed PPT [1]) representing the “optimal” or “best case” performance level and $12 \mu\text{Ns/J}$ to represent a “non-optimal” or “worst case” scenario.

Assuming now different values of the $\Delta m/E_1$ ratio (in the range of those reported in Table 2) and assuming that 90% of the total propellant mass will be used the total energy needed and total impulse delivered by the first stage can be calculated. These values are reported in Figure 4 together with the total impulse required by the mission.

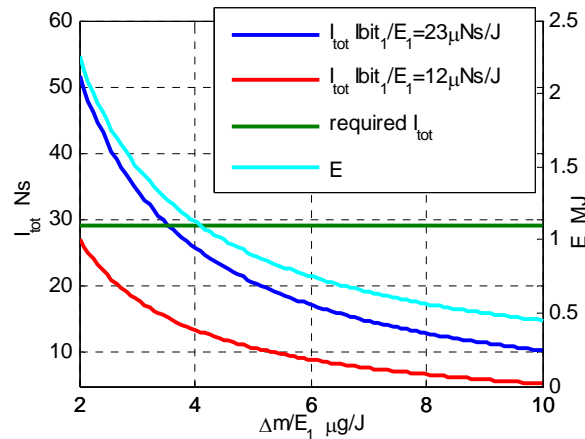


Figure 4: Impulse bit and energy needed to ablate all the propellant for different values of $\Delta m/E_1$

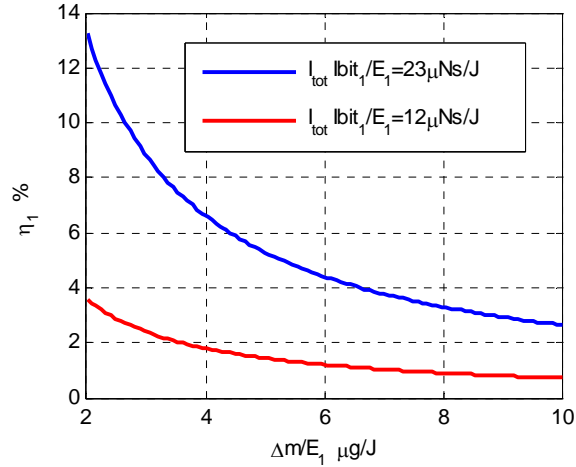


Figure 5: Efficiency for different I_{bit}/E_1 ratio as a function of $\Delta m/E_1$

Noting that a power of 0.3 W for one year corresponds to 9.46 MJ we can conclude that the thruster will confidently be able to utilize all the propellant. If the first stage of the thruster will work in its “optimal” conditions, delivering 23 $\mu\text{Ns}/\text{J}$, the mission can be accomplished even without the second stage, given that the mass ablated per unit of energy is below 3.5 $\mu\text{g}/\text{J}$. Looking at Table 2 and considering the chosen energy per area ratio of 2 J/cm^2 it can be seen that this assumption is reasonable and that the corresponding minimum efficiency is about 7%, also reasonable for a side-fed PPT according to Table 2. If these conditions do not apply, the second stage will be necessary to reach the required total impulse value of 28.4 Ns.

The $\Delta m/E_1$ ratio will also influence the number of shots needed to ablate all the propellant, hence the minimum allowable shot frequency. From this shot frequency the maximum energy per shot that can be used on the second stage can be calculated as

$$E_2 = \frac{P}{f} - E_1 \quad (2)$$

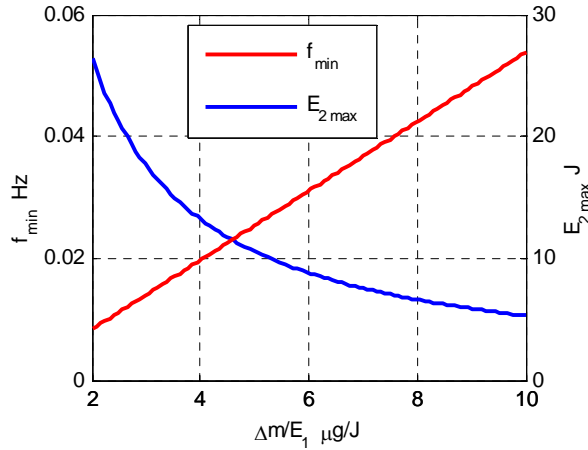


Figure 6: Minimum allowable shot frequency and maximum allowable energy on the second stage assuming to have 0.3 W of power available for 1 year

As we can see from Figure 6 the limits on minimum shot frequency and on the maximum energy we can use on the second stage are non-stringent, hence the choice of E_2 will be done on the basis of mass and performance consideration without worrying about the available power.

The second stage requirements will be derived starting from the data presented in Figure 4, assuming that 40% of the propellant is ablated in the form of LTA [2] and that the second stage discharge will involve only the LTA part of the ablated propellant. The value of the required impulse bit will be derived as a function of $\Delta m/E_1$ and then, assuming different values of the second stage shot energy, the required thrust efficiency will be calculated.

The shot energies used in the calculations will be 4, 3, 2 and 1 J, where the maximum value has been fixed to 4 J because the shot energy will drive the size and mass of the capacitor and considering the strict mass limitation of the whole project.

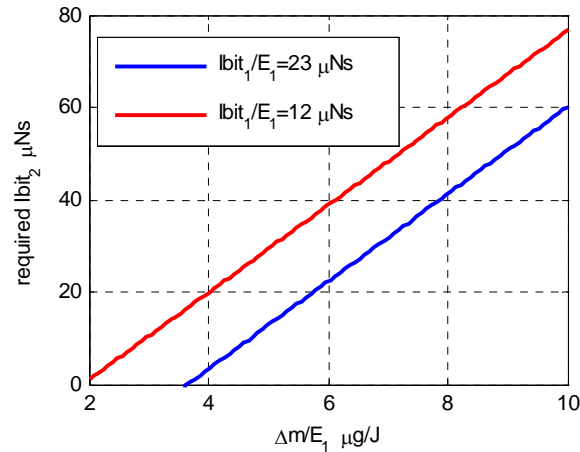


Figure 7: Required impulse bit from the second stage as a function of $\Delta m/E_1$ for different I_{bit_1}/E_1 ratio.

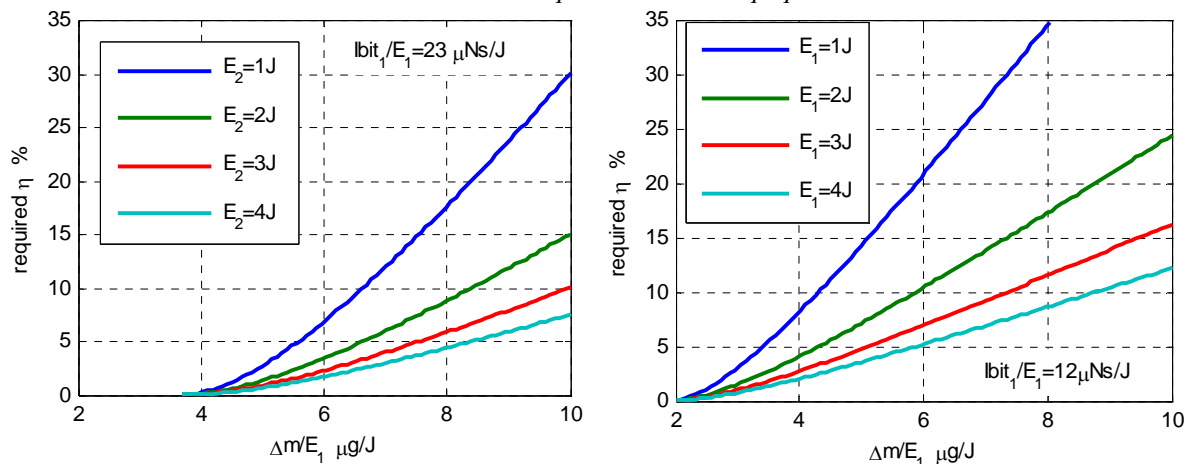


Figure 8: Required value of second stage efficiency as a function of E_2 for different values of I_{bit_1}/E_1 .

Looking at Figure 8 we will baseline an energy of 4J for the second stage and we will focus the design on maximizing the stage efficiency. In particular, we can see that if an efficiency of 5% is achieved the thruster will meet the mission requirements for any $\Delta m/E_1$ ratio lower than 6 $\mu\text{g}/\text{J}$ (assuming that the I_{bit_1}/E_1 ratio does not fall below 12 $\mu\text{Ns}/\text{J}$).

C. Second Stage Design

The ideal function of the second stage is to discharge over the LTA portion of the propellant to accelerate it. The LTA portion of the propellant will reach the second stage in a gaseous form (even if also macro particles will be present) hence this stage may be preliminarily treated as a gas-fed PPT. The design of this stage will be then based on the gas-fed PPT model developed at Princeton University by J. Ziemer [11, 12, 16, 17] even though this model does not take into account gas-dynamic effects, focusing only on the electromagnetic component of the thrust.

1. Capacitor choice

In Ziemer's model the performance of a gas-fed PPT is related to a limited number of non-dimensional parameters. The ones of more importance to us are the dynamic impedance parameter α and the critical resistance ratio ψ

$$\alpha = \frac{L^3 V_0^2 C^2}{18 L_0^2 m'} \quad (3)$$

$$\psi = \frac{R}{2} \sqrt{\frac{C}{L_0}} \quad (4)$$

where m' is the linear density of the gaseous propellant. Assuming that the gas has a constant distribution inside the PPT channel before the discharge is initiated the thruster efficiency has been found to scale as

$$\eta \propto \frac{\alpha}{\psi^4} = \frac{8 L^3 V_0^2}{9 R^4 m'} \quad (5)$$

Hence we ideally want to maximize α and to minimize the critical resistance ratio. Unfortunately the smaller is ψ the more oscillatory the discharge becomes hence the more energy is dissipated on the electrodes and capacitor resistance, therefore reducing the total efficiency. Ideally to optimize the energy transfer to the propellant we would like to have a critically damped discharge and hence $\psi = 1$.

The other parameters we can work on to maximize the efficiency are the inductance per unit length and the capacitor voltage. As already explained above the inductance per unit length depends on the geometry of the thruster and in particular on the h/w ratio. The considerations regarding the h/w ratio for the first stage are also valid for the second one hence this ratio will be kept equal to 2.

The discharge voltages commonly used in gas-fed PPTs are normally of the order of 200-300 V. According to Eq. 5 increasing this value would produce an increase in efficiency but this will also produce an increase in the capacitor mass and/or in the stored energy (if the capacitor capacity is kept unchanged). Considering the project strict mass budget and considering that we would like to be close to a critically damped discharge our baseline choice is to use a capacitor of 32 μ F with a voltage of about 500V. A market search to check the mass of such a capacitor is still ongoing; if the mass is found to be too high the voltage might be increased to reduce the required capacitance, if this is not sufficient the energy on the second stage will be reduced.

2. Electrode design

An important factor affecting the efficiency is the length of the electrodes. In [12] it has been shown how an optimal electrode length exists. In particular, if the electrodes are too short the propellant is expelled when there is still energy stored in the capacitor whereas if the electrodes are too long the friction with the walls will slow down the propellant. In this project, given the tight constraints on the dimensions, we will most probably fall in the first case with the electrode length being too short. Considering the length of the first stage and considering that an insulating separator between the two stages must be taken into account to avoid cross discharging between the two stages the maximum length for the second stage electrodes is 1.4 cm.

Another factor affecting the efficiency is the presence of sidewalls. Sidewalls will help the energy transfer process constraining the propellant in the electrode zone but they will also slow down the propellant due to friction. According to the experimental results found in [11] the net effect of sidewalls over a parallel plate gas-fed PPT is negative reducing the value of I_{bit} and I_{sp} . Considering that in our case side walls are needed to avoid propellant contamination of the electronics we will place the side walls with a divergence angle of 30°. To maximize the gas-dynamic thrust component of the second stage also the electrodes will have a divergence angle of 30°. To maintain an h/w ratio close to 2 the electrode shape will be trapezoidal, with width increasing towards the downstream end of the thruster.

3. Secondary discharge timing

Another important parameter to define is the delay between the first and the second discharge. Ideally, after the main discharge on the first set of electrodes a train of short pulses will be sent to the secondary electrode to accelerate all the LTA [5]. Unfortunately the electronics needed to form such a train of pulses is far too heavy for this project, hence only one pulse will be used.

Regarding the timing of this pulse there are two possibilities. The first one consists in letting the plasma produced by the first stage trigger the secondary discharge, in this case a capacitor with a high value of capacitance will be used so that the discharge will last until the LTA portion of the propellant reaches the second set of electrodes. The second possibility consists in using a timed switch and to arbitrarily choose the delay time.

The first option is easier since there is no need for a switch but, since the second discharge will be triggered by the fastest portion of the plasma produced by the first stage, and since this part of the plasma has been found to

travel at about 30Km/s [18-21], the delay between the second discharge triggering and the arrive of the LTA will be significant hence the capacitance needed will be very high resulting in a very heavy capacitor.

If a smaller capacitor is used the discharge will not last enough, hence all the energy will be deposited in the fastest portion of the plasma produced by the first stage. Considering the high velocity of this portion of the propellant, the energy required to further accelerate it will be very high drastically affecting the efficiency. Considering all these we decided to use a switch to trigger the second stage discharge.

The delay between the two discharges must be defined based on the speed of the LTA. The LTA is produced after the main discharge ends and can be reasonably expected to travel with a thermal velocity correspondent to the Teflon[®] sublimation temperature. Considering that this temperature is about 600 K the LTA velocity will be about 500-600 m/s. Given that the first stage capacitor has a capacitance of 3 μ F and assuming a resistance of about 0.1 Ω with an initial inductance of the order of 10 nH the first stage discharge will last about 7 μ s. Assuming that the LTA will travel at 550 m/s the second stage will be filled by the LTA propellant after about 45 μ s.

Since many assumptions have been made to determine the value of the delay between the first and second discharge and since the time needed for the LTA to fill the second stage depends on the real functioning of the thruster we plan to use at least 3 different time delays during tests to empirically find the one that is producing the best performances. The delays to be used will be 30, 50 and 80 μ s.

D. Spark Plug Design

Two spark plugs will be needed by the thruster, one for each stage. The main difficulty in the design of the spark plugs for this thruster is the small dimensions of the electrodes. Spark plugs have normally a concentric design [22] with a central electrode connected to a high voltage supply (up to about 10kV) surrounded by a layer of semiconductor material (or Teflon[®]) and are inserted in one of the thruster electrodes as shown in Figure 9.

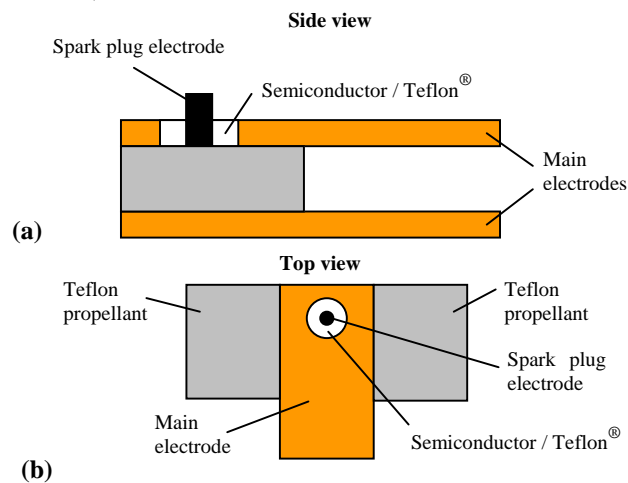


Figure 9: Diagram of a “conventional” spark plug setup: (a) side view, (b) top view.

In such a setup the discharge may happen at any point along the electrode/semiconductor circumference. This is tolerable and will cause small shot to shot variation given that the propellant length is much bigger than the spark plug size. In the case of our HFB-PPT thruster, the propellant length is 3.5 mm and if the spark plug is much smaller than this, it would be extremely small and therefore difficult to manufacture. To overcome this problem a rectangular spark plug has been designed. A sketch with the most important dimensions is reported below.

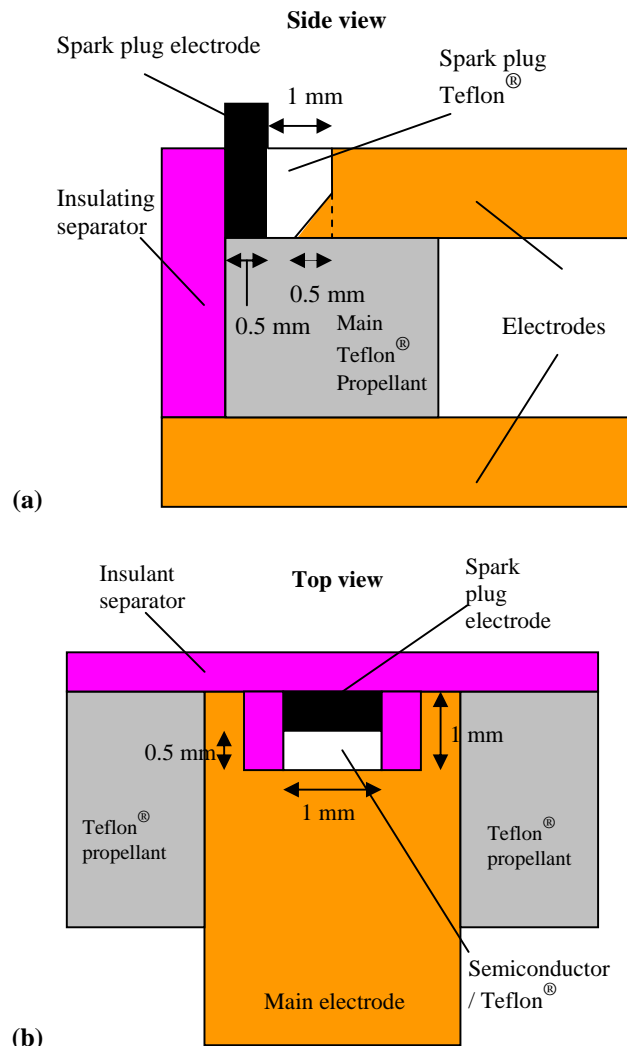


Figure 10: Spark plug diagram: (a) Side view, (b) top view.

The main electrode will be manufactured in tungsten and the chamfer in the thruster electrode has been introduced to provide the discharge a preferential attachment point and to retain the Teflon. With this design the discharge will occur somewhere along the spark plug electrode width but will be localised at the beginning of the main propellant bar (0.5 mm from its edge) hence assuring that the main discharge will sweep along the whole propellant face.

Another important factor to take into account is the polarity of the spark plug and of the electrodes. As reported in [23] the choice of the respective polarities of the spark plug and of the main electrodes will strongly influence the presence of carbonization on the propellant surface. In particular, according to what is reported in [23] the presence of carbonization will be minimized with the spark plug inserted into the ground electrode and charged to a positive voltage whereas the voltage between the electrodes is negative.

To confirm this, the computed electric field lines are reported below for two different values of the main electrode voltage, corresponding to +1kV and -1kV.

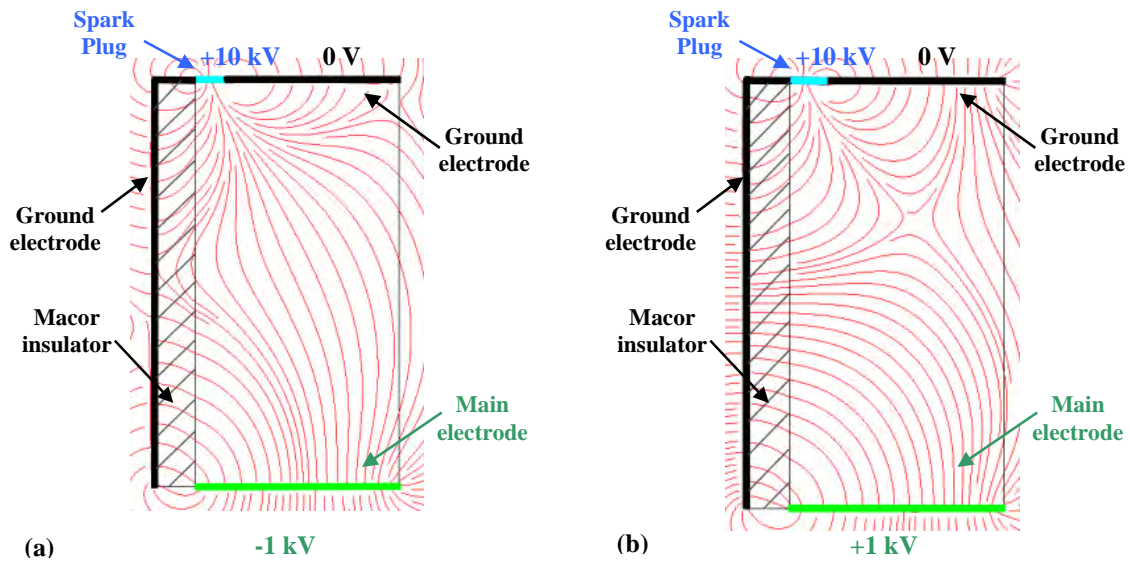


Figure 11: Electric field lines for different voltage configurations

As shown, when the spark plug voltage and the main electrode voltage are of opposite sign, Figure 11 (a), the electric field lines are more vertical than when the potentials are of the same sign, Figure 11 (b). When the spark plug strikes, the discharge will initially follow the direction of the electric field lines hence the more vertical the lines are the closer to the back of the thruster the discharge will attach, consequently sweeping the whole face of the propellant and limiting the carbonization that occurs when the discharge does not efficiently sweep all the propellant face. Considering this, we will baseline a configuration like the one in Figure 11 (a) and we will use a spark plug discharge energy of 0.1 J, with voltages up to 15kV.

IV. Thruster assembly

A 3D view of how the thruster discharge chamber will look like and a cross section of the thruster are shown below in Figure 12 and Figure 13.

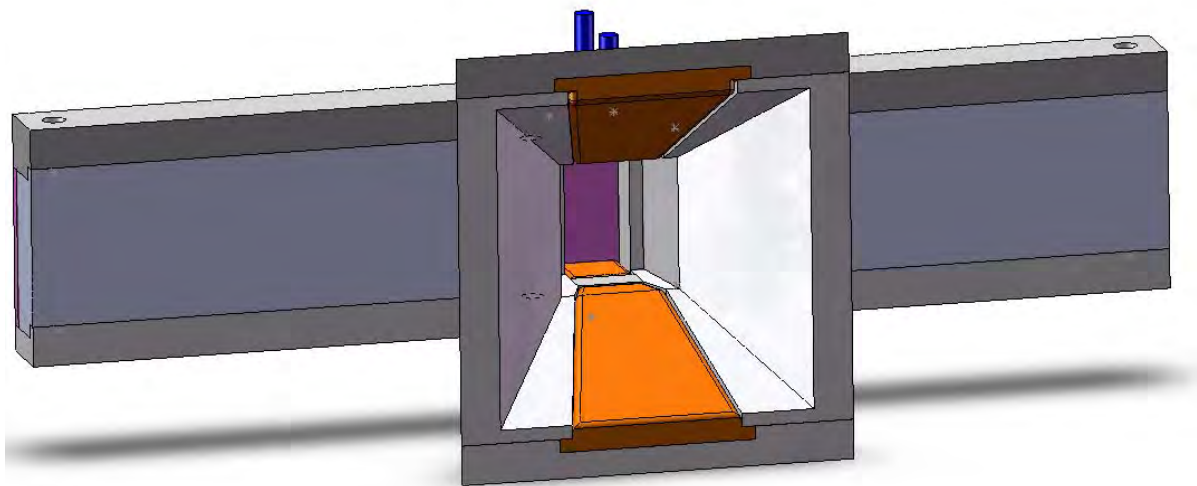


Figure 12: 3D view of the HFB-PPT discharge chamber

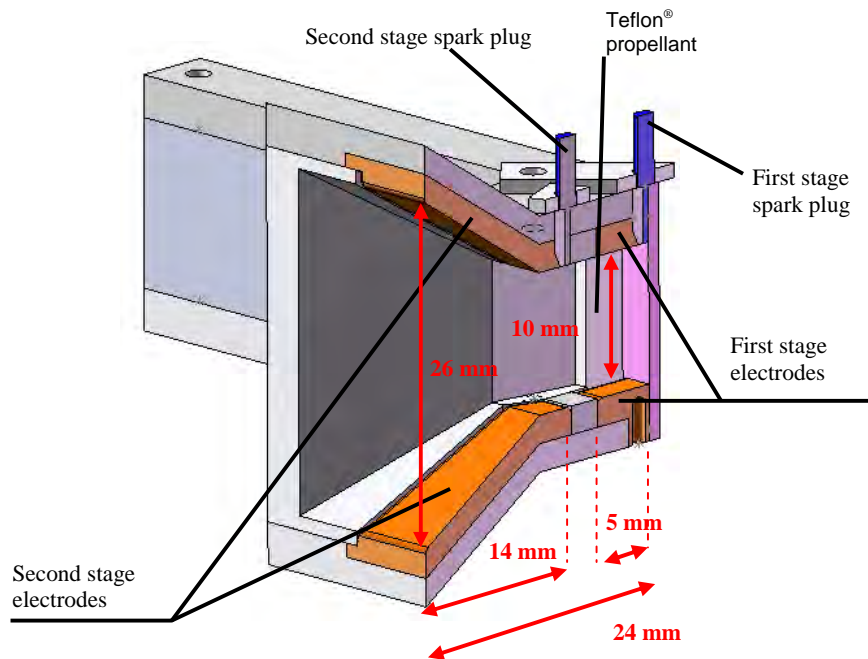


Figure 13: Section of the HFB-PPT discharge chamber

As it can be seen from Figure 12 the thruster electrodes are completely covered by a machinable glass ceramic (MACOR[®]) layer, as an insulation method. The design of the thruster parts has been done to minimize the total mass and to have a modular thruster assembly where every part can be easily substituted.

According to the present design, the mass of the discharge chamber is 35g, including the propellant mass.

V. Conclusion and future work

The design of a two stage Pulsed Plasma Thruster for Cubesat application has been presented. The ultimate goal of this project is to design an HFB-PPT able to double the lifetime of a Cubesat on a 600-km orbit. The first stage of the thruster has been designed to maximize its performance to ideally be able to meet the mission requirements without the need of a second stage. This has been done to add a degree of redundancy in the design and because the impulse bit improvement related to the use of a second stage has still not been experimentally quantified. From an analysis on the expected first stage performance the second stage requirements have been formulated. The design of the two spark plugs used was also presented.

Future work will consist in building the thruster and testing it to assess its performance and durability. Tests will include vibration tests, thermo-vacuum tests and measurements of discharge currents, mass bit and impulse bit using different delays between the first and the second discharges.

References

- [1] R.L.Burton and P.J.Turchi, "Pulsed Plasma Thruster", Journal of Propulsion and Power, Vol. 14, No. 5, 1998.
- [2] G.G.Spanjers, J.S.Lotspeich, K.A.McFall, and R.A.Spores, "Propellant Losses Because of Particulate Emission in a Pulsed Plasma Thruster", Journal of Propulsion and Power, Vol. 14, No. 9, 1998.
- [3] G.G.Spanjers, K.A.McFall, F.S.Gulczynski, and R.A.Spores, "Investigation of propellant inefficiencies in a pulsed plasma thruster", AIAA, ASME, SAE, and ASEE, Joint Propulsion Conference and Exhibit, 32nd, LakeBuena Vista, FL, July 1-3, 1996.
- [4] R.Intini Marques and S.B.Gabriel, "High Frequency Burst Pulsed Plasma Thruster Research at the University of Southampton", 30th International Electric Propulsion Conference, Florence, Italy September 17-20, 2007.

- [5] R.Intini Marques and S.B.Gabriel, "*Improved Pulsed Plasma Thruster and Method of Operation Thereof*", Patent Number PCT/GB2007/003543,
- [6] R.Intini Marques, "*A Mechanism to Accelerate the Late Time Ablation for the Pulsed Plasma Thruster*", Ph.D.Thesis, Astronautic Research Group, School of Engineering Sciences, University of Southampton, UK, 2009.
- [7] D.J.Palumbo and W.J.Guman, "*Continuing Development of the Short Pulsed Ablative Space Propulsion System*", AIAA-SAE 8th Joint Propulsion Conference, New Orleans, 1972.
- [8] W.J.Guman, "*Designing Solid Propellant Pulsed Plasma Thruster*", 11th Electric Propulsion Conference, 1975.
- [9] P.Gessini and G.Paccani, "*Ablative Pulsed Plasma Thruster System Optimization for Microsatellites*", 27th International Electric Propulsion Conference, IEPC-01-182, 2001.
- [10] P.Gessini, R.Intini Marques, S.B.Gabriel, and S.M.Veres, "*Propulsion System Optimization for Satellite Formation Flying*", 4th International Workshop on Satellite Constellations and Formation Flying, INPE, São José dos Campos, Brazil, 2002.
- [11] J.Ziemer, E.Y.Choueiri, and D.Birx, "*Comparing the Performance of Co-Axial and Parallel-Plate Gas-Fed PPTs*", 26th International Electric Propulsion Conference, 1999.
- [12] J.Ziemer, "*Performance Scaling of Gas-Fed Pulsed Plasma Thrusters*", Ph.D.Thesis, Department of Mechanical and Aerospace Engineering, Princeton University, 2001.
- [13] R.L.Burton, M.J.Wilson, and S.Bushman, "*Energy Balance and Efficiency of the Pulsed Plasma Thruster*", AIAA/ASME/SAE/ASEE Joint Propulsion Conference and Exhibit, 34th, Cleveland, OH, July 13-15, 1998.
- [14] I.Kohlberg and W.O.Coburn, "*A Solution for Three Dimensional Rail Gun Current Distribution and Electromagnetic Fields of a Rail Launcher*", IEEE Transactions on Magnetics, 31, pag. 628-633, 1995.
- [15] R.Jahn, "*Physics of Electric Propulsion*", McGraw-Hill, New York, 1968.
- [16] J.Ziemer and E.Y.Choueiri, "*A Characteristic Velocity for Gas-Fed PPT Performance Scaling*", AIAA/ASME/SAE/ASEE Joint Propulsion Conference and Exhibit, 36th, Huntsville, AL, July 16-19, AIAA-2000-3432, 2000.
- [17] J.Ziemer and E.Y.Choueiri, "*Scaling Laws for Electromagnetic Pulsed Plasma Thrusters*", Plasma Sources Sci.Technol., 10, pag. 395-405, 2001.
- [18] N.Antropov, L.Gomilka, G.Diakonov, I.Krivososov, G.Popov, and M.Orlov, "*Parameters of Plasmoid Injected by PPT*", AIAA Paper 97-2921, 1997.
- [19] W.J.Guman, R.J.Vondra, and K.Thomassen, "*Pulsed Plasma Propulsion System Studies*", AIAA Paper 70-1148, 1970.
- [20] M.Hirata and H.Marakami, "*Exhaust Gas Analysis of a Pulsed Plasma Engine*", AIAA Paper 84-52, 1984.
- [21] R.Eckman, N.Gatsonis, R.Myers, and E.Pencil, "*Experimental Investigation of the LES 8/9 Pulsed Plasma Thruster Plume*", 25th International Electric Propulsion Conference, IEPC 97-126, 1997.
- [22] M.E.Brady and G.Aston, "*Pulsed Plasma Thruster Ignitor Plug Ignition Characteristics*", Journal of Spacecraft and Rockets, Vol. 20, No. 5, 1983.
- [23] R.J.Vondra and K.Thomassen, "*Performance Improvements in Solid Fuel Microthrusters*", Journal of Spacecraft and Rockets, Vol. 9, No. 10, 1972.